	Amorphous Si	Poly-Si	Organic
Status	Mature	Development	Research
TFT type	N-TFT	N-TFT or P-TFT	P-TFT or N-TFT
Mobility (cm^2/Vs)	0.1-1.0	50-200	0.005-3
Uniformity	Good	Poor	Unknown
Stability	Poor	Good	Unknown
Cost	Low	High	Very low
Ion/Ioff	$>10^6$	$>10^6$	10^3-10^8
Size and voltage to drive 10μA (Gate dielectric is 300nm and channel length is 5μm) (W=channel width)	W=92μm (V_{GS}-V_{TH})=7V	W=10μm (V_{GS}-V_{TH})=1.5V	W=181μm (V_{GS}-V_{TH})=25V

Table 1.1 Comparisons of TFTs using different materials

	TC	**BC**	**TBC**
R_c (M ohm)	**0.38**	**19.1**	**10.4**

Table 3.1 Contact resistance in TC, BC, and TBC OTFTs

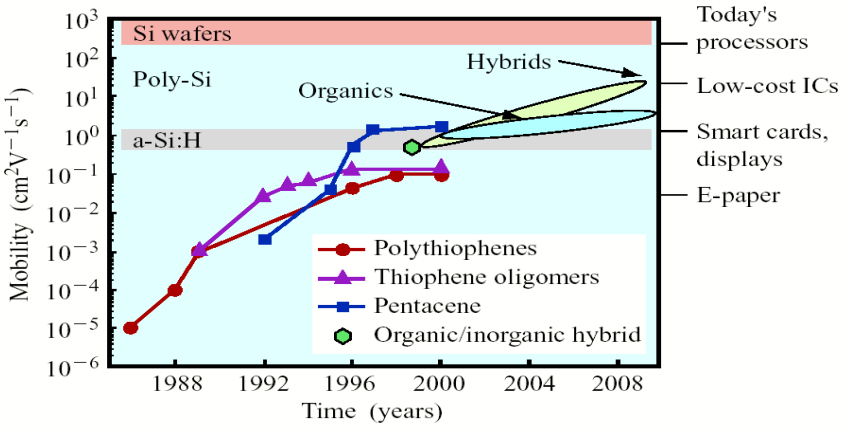

Fig. 1.1 Mobility of the organic semiconductors has been improved by five orders of magnitude over the past 15 years.

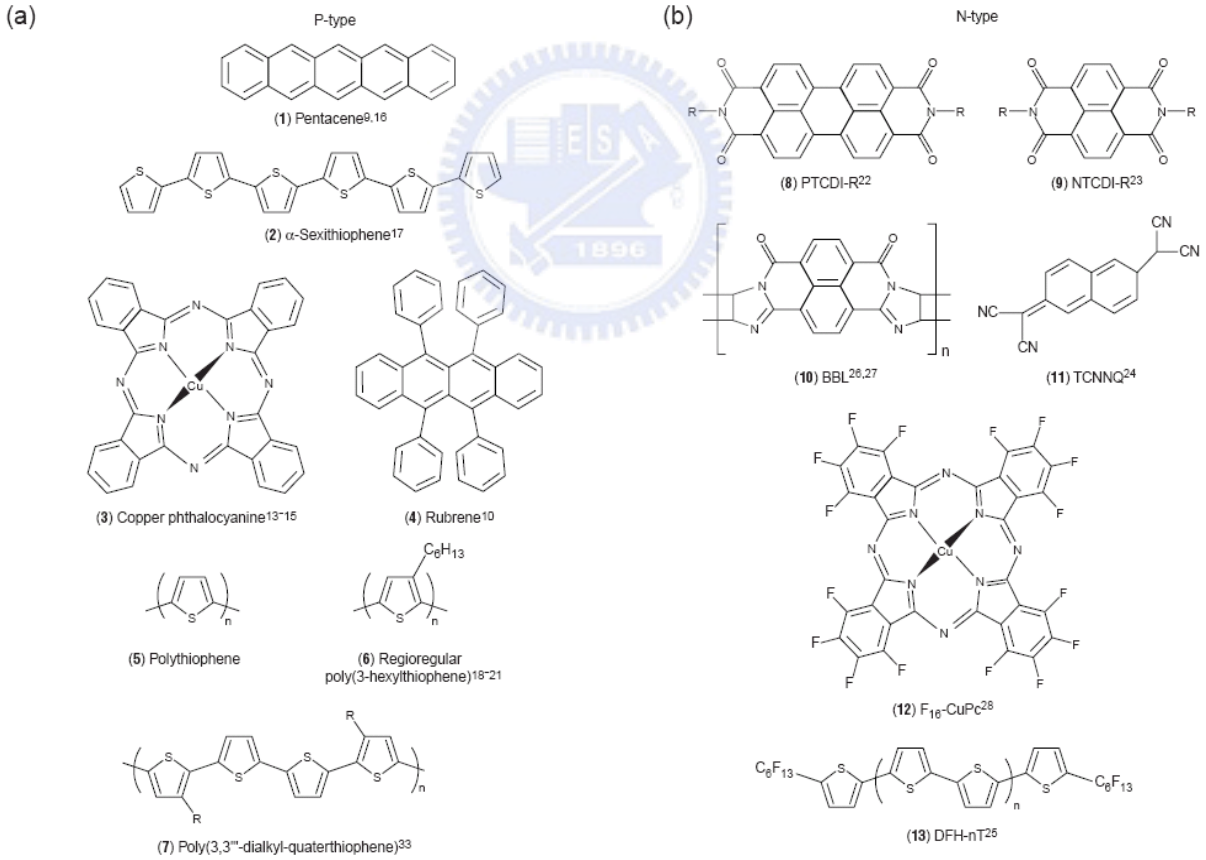

Fig. 1.2 Prominent (a) p-type and (b) n-type organic semiconductor materials

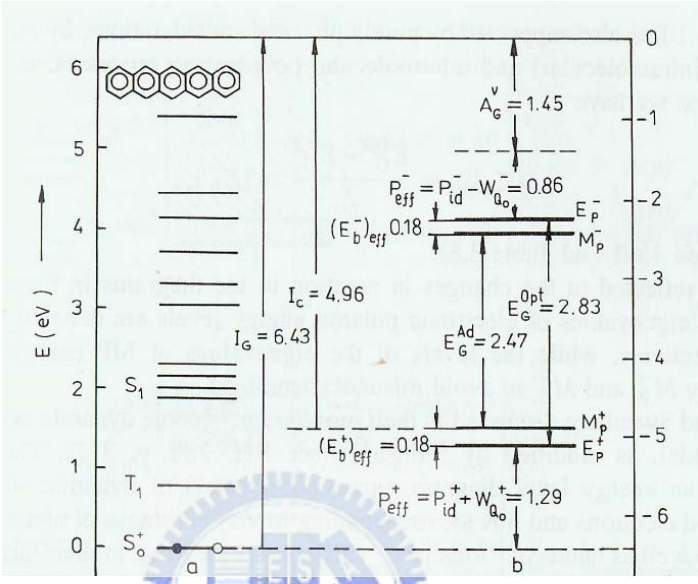

Fig. 1.3 Energy band diagram of pentacene.

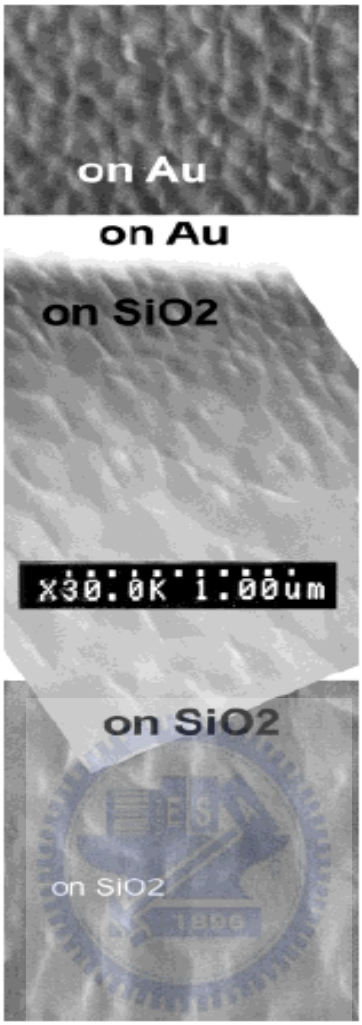

Fig. 1.4 Scanning electron microscopy (SEM) image of a pentacene thin film grown on SiO_2 and a Au electrode. The grain size is much smaller on Au than on SiO_2 far from the Au edge. Pentacene grain size on SiO_2 in the region close to the Au edge is similar to that on Au and increases with increasing distance from the edge. Reprinted from [19].

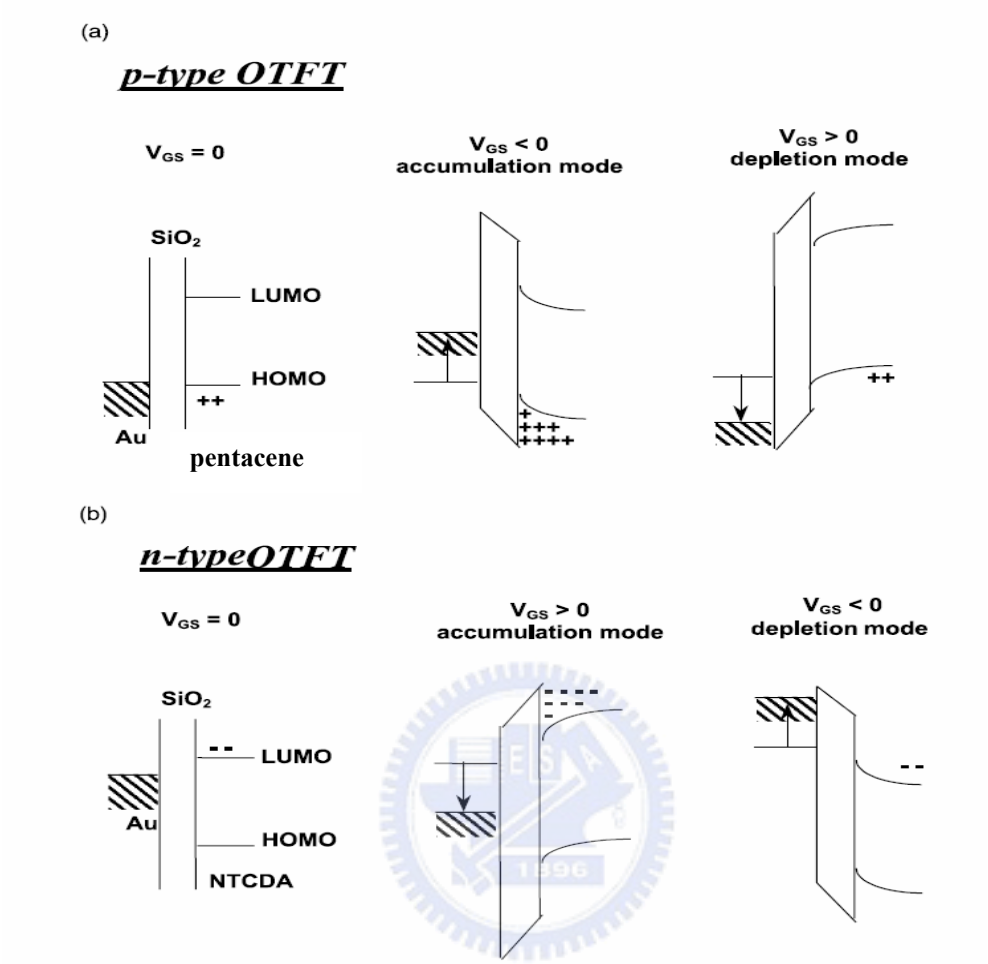

Fig. 1.5 Energy band diagrams (a) for a p-channel (pentacene) and (b) for a n-channel (NTCDA) OTFTs. The left side shows the devices at zero gate bias, while in the centre and in the right part the accumulation and depletion mode operation regimes are presented [25].

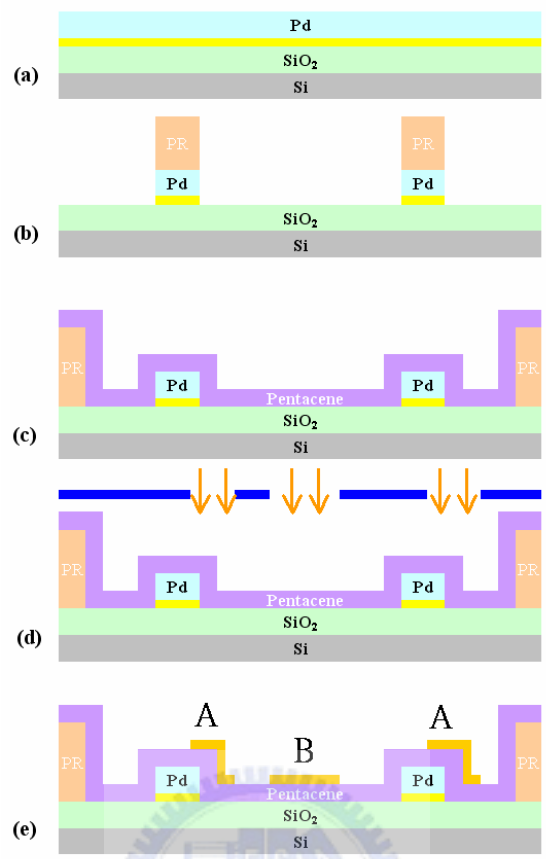

Fig. 2.1 Structure and process flow of vertical organic thin film transistors

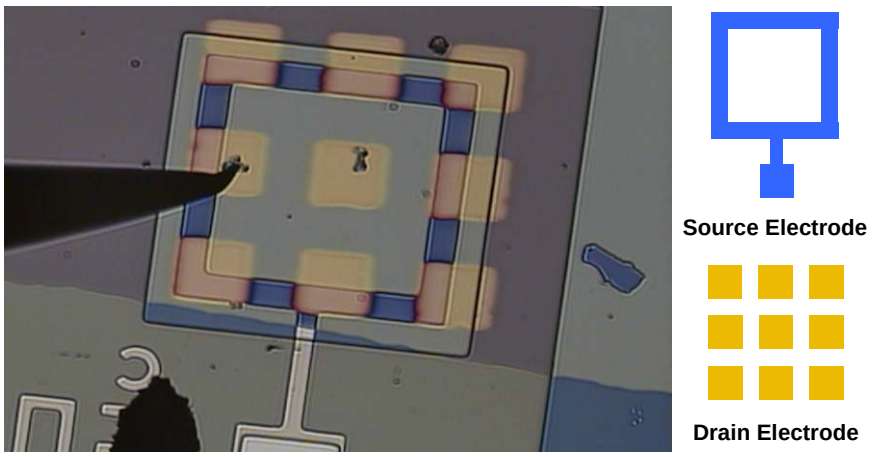

Fig. 2.2 Top view microscope image of VOTFTs. The shapes of source/drain electrodes are also shown.

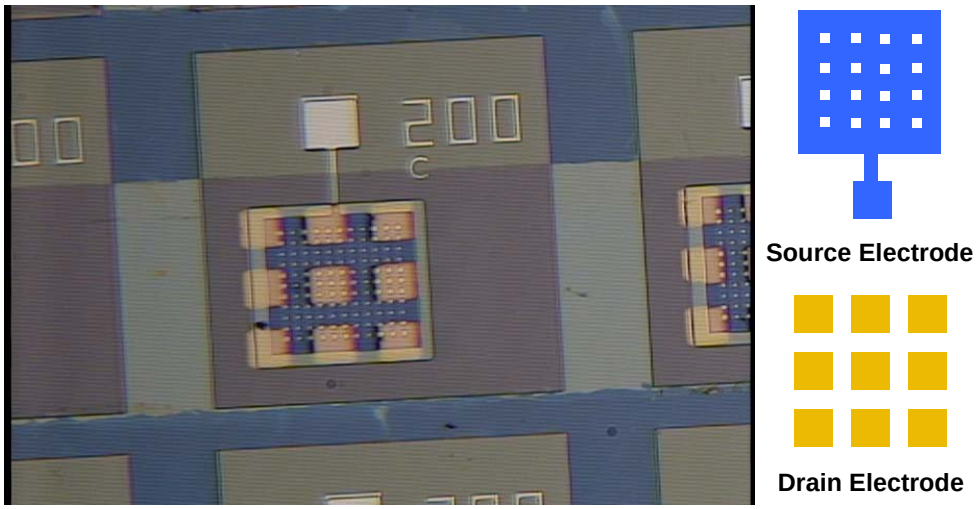

Fig. 2.3 Top view microscope image of VOTFTs with meshed source electrode

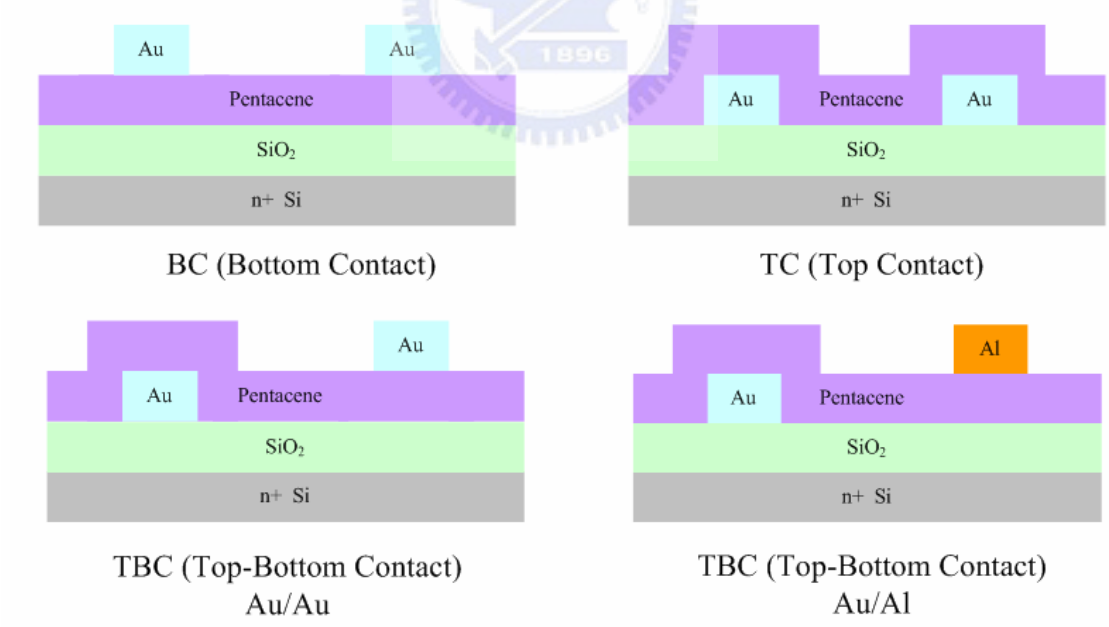

Fig. 2.4 OTFTs with BC TC TBC

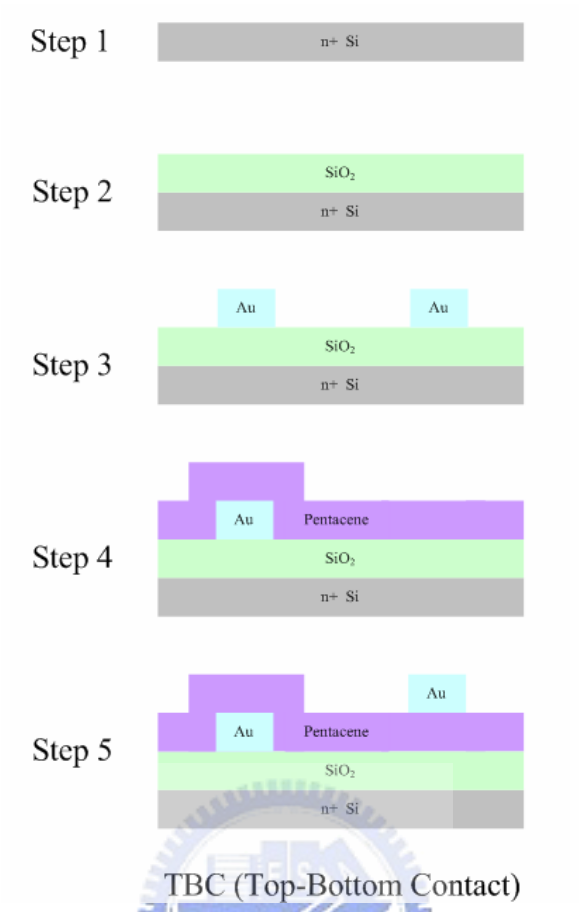

Fig. 2.5 Process flow of TBC OTFTs

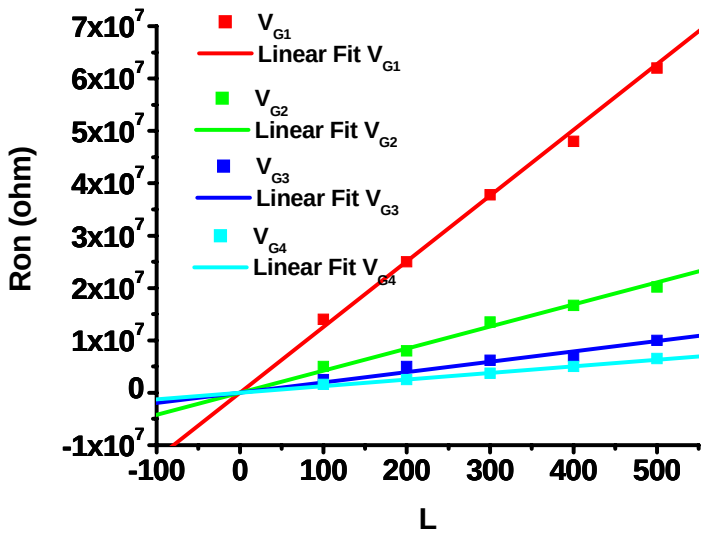

Fig. 2.6 Device resistance R as a function of channel length L at V_{DS} =-1V to −5V

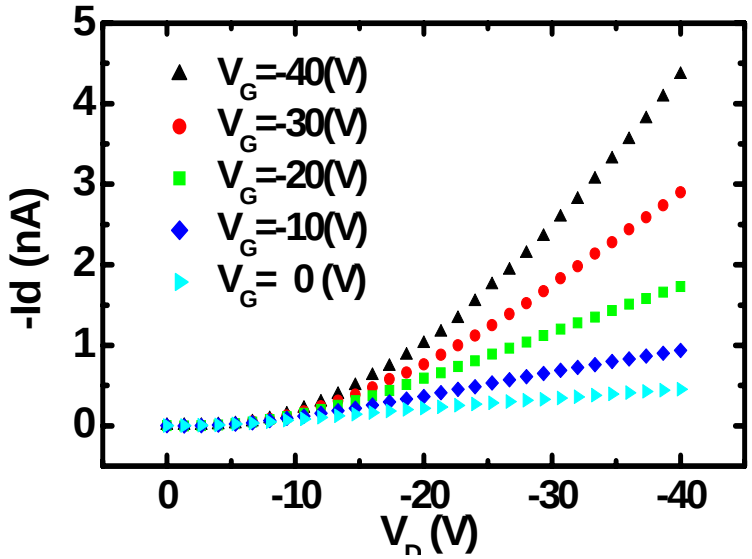

Fig. 3.1 Output characteristics of Group-A VOTFTs

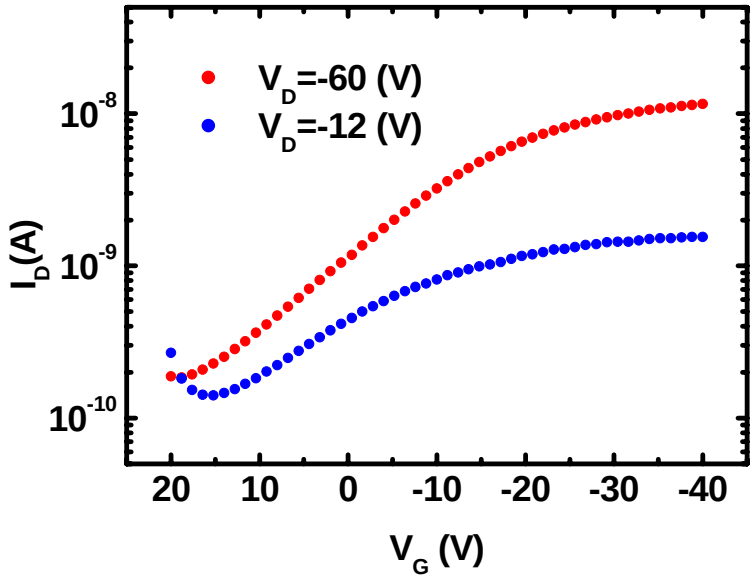

Fig. 3.2 Transfer characteristics of Group-A devices

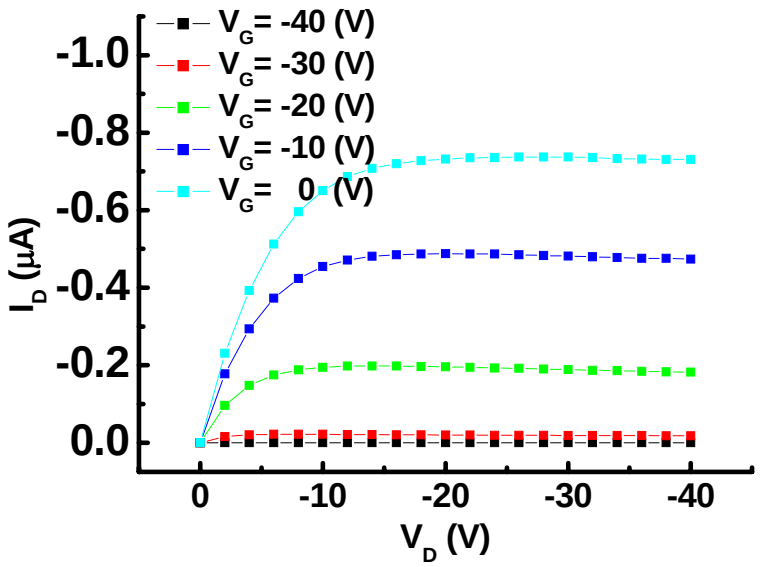

Fig. 3.3 Output characteristics of Group-B devices

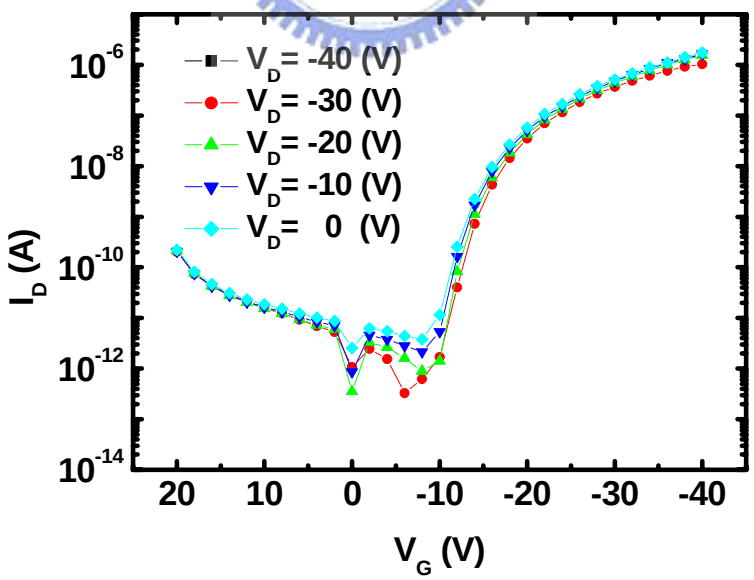

Fig. 3.4 Transfer characteristics of Group-B devices

(a)

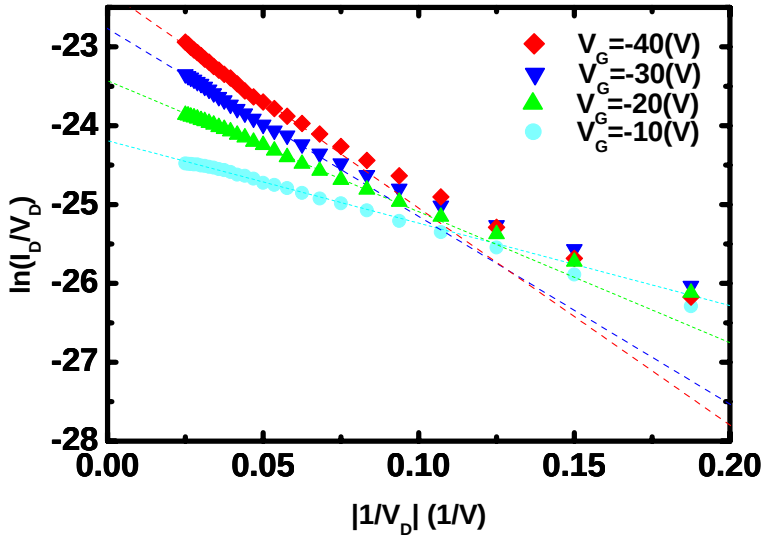

(b)

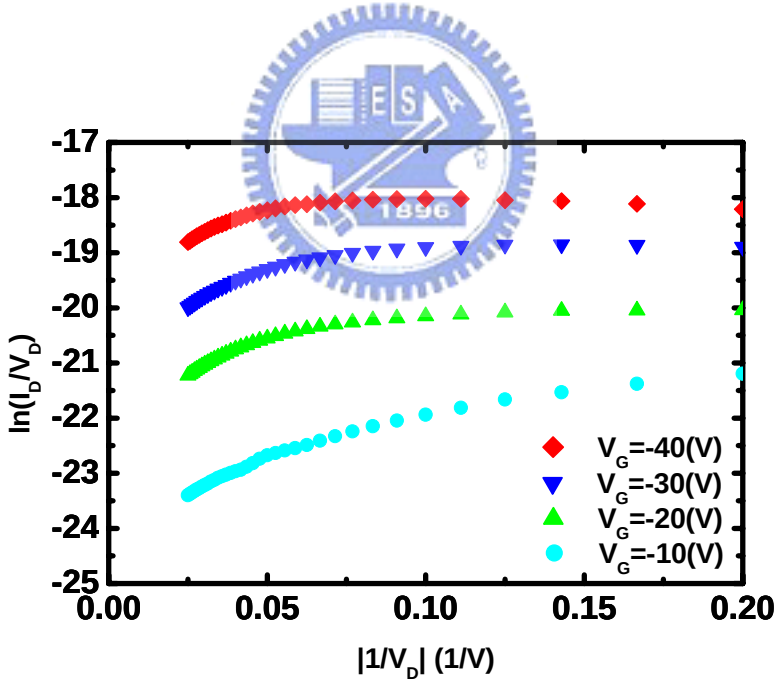

Fig. 3.5 $\ln(I_D/V_D)$ v.s. $1/|V_D|$ plots for: (a) Group-A devices with ultra short channel length and (b) Group-B devices with long channel length

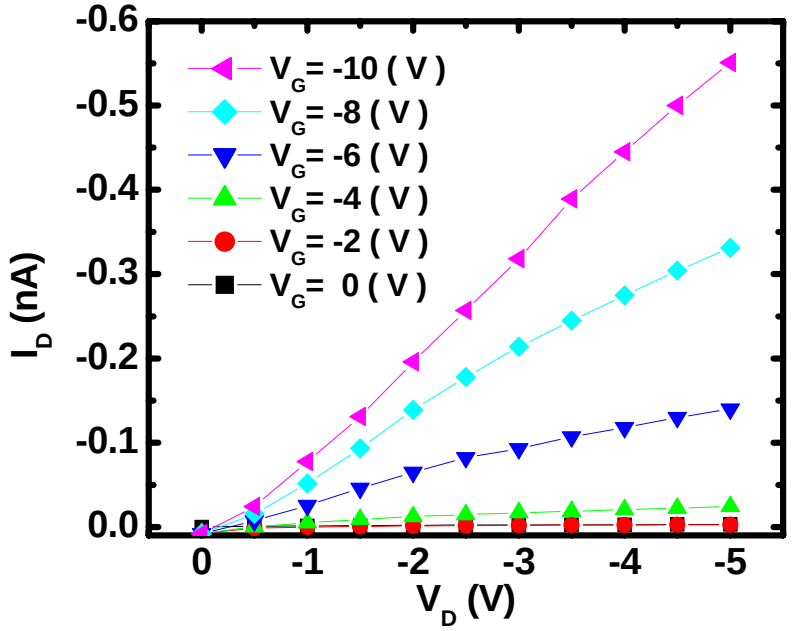

Fig. 3.6 Output characteristics of VOTFTs of meshed source electrode

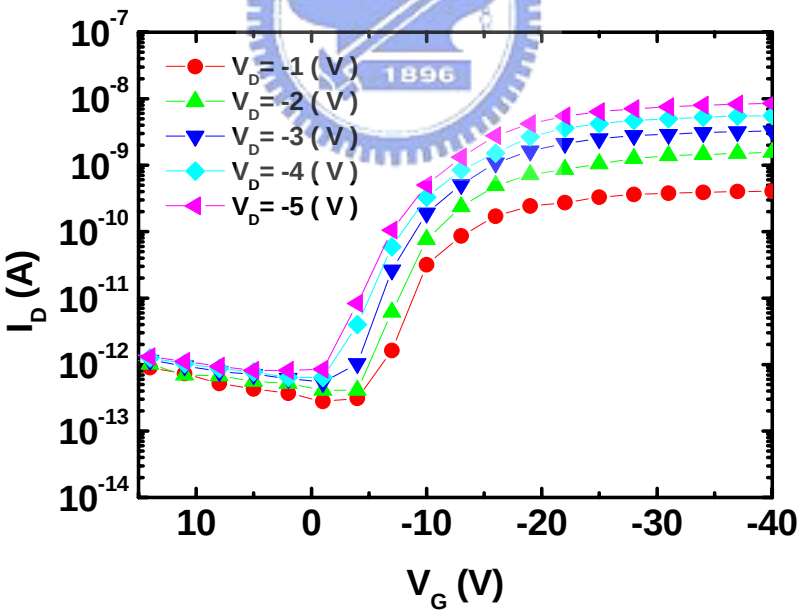

Fig. 3.7 Higher on/off current ratio transfer characteristics from meshed source VOTFTs